

AD-748-613

Plasma Wave Observations Near the
Plasmapause with the S3-A Satellite*

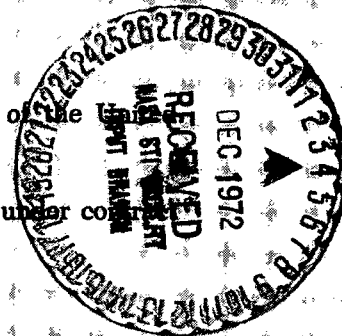
by

Roger R. Anderson and Donald A. Gurnett



Reproduction in whole or in part is permitted for any purpose of the United States Government.

Research was sponsored in part by the Office of Naval Research under contract N00014-68-A-0196-0003.



Department of Physics and Astronomy
THE UNIVERSITY OF IOWA

Iowa City, Iowa

(NASA-CR-129243) PLASMA WAVE OBSERVATIONS
NEAR THE PLASMAPAUSE WITH THE S3-A
SATELLITE R.R. Anderson, et al (Iowa
Univ.) Jul. 1972 27 p
AD-748-613 N73-12388
CSCL 04A G3/13 48021
Unclas

Plasma Wave Observations Near the
Plasmapause with the S³-A Satellite*

by

Roger R. Anderson and Donald A. Gurnett

Department of Physics and Astronomy
The University of Iowa
Iowa City, Iowa 52240

July 1972

REPRODUCTION IN WHOLE OR IN PART IS PERMITTED FOR ANY PURPOSE OF
THE UNITED STATES GOVERNMENT.

*This research was supported in part by the National Aeronautics and
Space Administration under contracts NAS5-11167 and Grant NGL-16-001-043
and the Office of Naval Research under Grant N00014-68-A-0196-0003.

DOCUMENT CONTROL DATA - R&D

(Security classification of title, body of abstract and indexing annotation must be entered when the overall report is classified)

1. ORIGINATING ACTIVITY (Corporate author) Department of Physics & Astronomy University of Iowa		2a. REPORT SECURITY CLASSIFICATION UNCLASSIFIED	
		2b. GROUP	
3. REPORT TITLE "Plasma Wave Observations Near the Plasmopause with the S ³ -A Satellite"			
4. DESCRIPTIVE NOTES (Type of report and inclusive dates) Progress, July 1972			
5. AUTHOR(S) (Last name, first name, initial) Anderson, Roger R. and Donald A. Gurnett			
6. REPORT DATE July 1972		7a. TOTAL NO. OF PAGES 26	7b. NO. OF REFS 10
8a. CONTRACT OR GRANT NO. N00014-68-A-0196-0003		9a. ORIGINATOR'S REPORT NUMBER(S) U of Iowa 72-19	
b. PROJECT NO.		9b. OTHER REPORT NO(S) (Any other numbers that may be assigned this report)	
c.			
d.			
10. AVAILABILITY/LIMITATION NOTICES Approved for public release; distribution is unlimited			
11. SUPPLEMENTARY NOTES		12. SPONSORING MILITARY ACTIVITY Office of Naval Research	
13. ABSTRACT [See following page]			

14. KEY WORDS	LINK A		LINK B		LINK C	
	ROLE	WT	ROLE	WT	ROLE	WT
Plasmopause Electric Field Noise VLF Radio Noise						

INSTRUCTIONS

1. **ORIGINATING ACTIVITY:** Enter the name and address of the contractor, subcontractor, grantee, Department of Defense activity or other organization (*corporate author*) issuing the report.
- 2a. **REPORT SECURITY CLASSIFICATION:** Enter the overall security classification of the report. Indicate whether "Restricted Data" is included. Marking is to be in accordance with appropriate security regulations.
- 2b. **GROUP:** Automatic downgrading is specified in DoD Directive 5200.10 and Armed Forces Industrial Manual. Enter the group number. Also, when applicable, show that optional markings have been used for Group 3 and Group 4 as authorized.
3. **REPORT TITLE:** Enter the complete report title in all capital letters. Titles in all cases should be unclassified. If a meaningful title cannot be selected without classification, show title classification in all capitals in parenthesis immediately following the title.
4. **DESCRIPTIVE NOTES:** If appropriate, enter the type of report, e.g., interim, progress, summary, annual, or final. Give the inclusive dates when a specific reporting period is covered.
5. **AUTHOR(S):** Enter the name(s) of author(s) as shown on or in the report. Enter last name, first name, middle initial. If military, show rank and branch of service. The name of the principal author is an absolute minimum requirement.
6. **REPORT DATE:** Enter the date of the report as day, month, year, or month, year. If more than one date appears on the report, use date of publication.
- 7a. **TOTAL NUMBER OF PAGES:** The total page count should follow normal pagination procedures, i.e., enter the number of pages containing information.
- 7b. **NUMBER OF REFERENCES:** Enter the total number of references cited in the report.
- 8a. **CONTRACT OR GRANT NUMBER:** If appropriate, enter the applicable number of the contract or grant under which the report was written.
- 8b, 8c, & 8d. **PROJECT NUMBER:** Enter the appropriate military department identification, such as project number, subproject number, system numbers, task number, etc.
- 9a. **ORIGINATOR'S REPORT NUMBER(S):** Enter the official report number by which the document will be identified and controlled by the originating activity. This number must be unique to this report.
- 9b. **OTHER REPORT NUMBER(S):** If the report has been assigned any other report numbers (*either by the originator or by the sponsor*), also enter this number(s).
10. **AVAILABILITY/LIMITATION NOTICES:** Enter any limitations on further dissemination of the report, other than those

imposed by security classification, using standard statements such as:

- (1) "Qualified requesters may obtain copies of this report from DDC."
- (2) "Foreign announcement and dissemination of this report by DDC is not authorized."
- (3) "U. S. Government agencies may obtain copies of this report directly from DDC. Other qualified DDC users shall request through _____."
- (4) "U. S. military agencies may obtain copies of this report directly from DDC. Other qualified users shall request through _____."
- (5) "All distribution of this report is controlled. Qualified DDC users shall request through _____."

If the report has been furnished to the Office of Technical Services, Department of Commerce, for sale to the public, indicate this fact and enter the price, if known.

11. **SUPPLEMENTARY NOTES:** Use for additional explanatory notes.
12. **SPONSORING MILITARY ACTIVITY:** Enter the name of the departmental project office or laboratory sponsoring (*paying for*) the research and development. Include address.
13. **ABSTRACT:** Enter an abstract giving a brief and factual summary of the document indicative of the report, even though it may also appear elsewhere in the body of the technical report. If additional space is required, a continuation sheet shall be attached.

It is highly desirable that the abstract of classified reports be unclassified. Each paragraph of the abstract shall end with an indication of the military security classification of the information in the paragraph, represented as (TS), (S), (C), or (U).

There is no limitation on the length of the abstract. However, the suggested length is from 150 to 225 words.

14. **KEY WORDS:** Key words are technically meaningful terms or short phrases that characterize a report and may be used as index entries for cataloging the report. Key words must be selected so that no security classification is required. Identifiers, such as equipment model designation, trade name, military project code name, geographic location, may be used as key words but will be followed by an indication of technical context. The assignment of links, roles, and weights is optional.

ABSTRACT

In this paper we describe the electric field noise phenomena observed by the S³-A spacecraft near the plasmapause during the magnetic storm of December 16-17, 1971. The most striking and unusual feature of these storm time electric field observations is the occurrence of a region of intense low-frequency (20 Hz to 500 Hz) electrostatic noise bursts just outside the plasmapause boundary. These noise bursts occurred concurrent with the rapid decrease in $24.3 \leq E \leq 35.1$ keV ring current protons mirroring near the equator during this storm and may be responsible for the pitch angle diffusion and loss of these particles. The characteristics of other phenomena, such as whistlers, ELF hiss, and banded chorus, observed near the plasmapause during this period are also discussed.

I. INTRODUCTION

The charged-particle and magnetic field experiments on the Small Scientific Satellite, S³-A, have provided a comprehensive survey of the plasma and magnetic field variations during the December 16-17, 1971, magnetic storm, the results of which are presented in a companion set of papers. The purpose of this paper is to describe the electric field noise phenomena observed at selected periods during this storm by the University of Iowa electric field experiment on S³-A.

Of particular interest during this storm is the observation of anomalous proton pitch angle distributions near the inner edge of the ring current on orbit 99 [Williams et al., 1972]. As the satellite crosses into the plasmasphere at about $L = 3.4$ on this orbit, the low-energy ($24.3 \leq E \leq 35.1$ keV) proton intensities decrease rapidly and the pitch angle distribution, which was a normal loss cone type distribution outside the plasmopause, develops a pronounced minimum perpendicular to the local magnetic field. Williams et al. [1972] have attributed the initial change in the pitch angle distribution and the onset of the decrease in the proton intensities to pitch angle scattering by ion cyclotron turbulence as first suggested by Cornwall et al. [1970]. Cornwall et al. [1971] predicted wave frequencies for the ion cyclotron turbulence near the magnetic equator to be from 0.33

to 0.75 of the proton cyclotron frequency. The proton cyclotron frequency at the inbound plasmopause crossing of orbit 99 was about 13 Hz, indicating that the ion cyclotron turbulence should be at a frequency of about 4 Hz to 10 Hz. However, no magnetic field signals attributable to these ion cyclotron waves were detected with the search coil magnetometer experiment on S³-A on this orbit [Parady and Cahill, 1972]. Since no ion cyclotron turbulence was detected, our primary objective in this paper is to investigate the electric field noise phenomena in this region of anomalous pitch angle distributions in order to determine if an electrostatic instability, such as recently suggested by Coroniti et al. [1972], could be responsible for the observed pitch angle scattering.

II. INSTRUMENTATION

The satellite S³-A was launched from the San Marco Equatorial Range, Kenya, Africa, on November 15, 1971, into an eccentric equatorial orbit. The perigee altitude was 222 km, the apogee altitude was 27,031 km ($5.24 R_E$ geocentric), the inclination was 3.57 degrees, and the orbital period was 7 hours 49 minutes. S³-A was spin stabilized with the spin axis near the ecliptic plane. The electric dipole antenna on S³-A consists of two graphite coated spheres, 14 cm in diameter, mounted on booms such that the center-to-center distance between the spheres is 5.08 meters. Each sphere is connected to a high input impedance ($C_{in} \approx 10$ pf, $R_{in} \approx 50$ megohms) unity gain preamplifier mounted on the boom about half way between the center of the sphere and the center of the spacecraft. The axis of the electric dipole antenna is perpendicular to the spacecraft spin axis.

The electronics instrumentation for the University of Iowa electric field experiment consists of two principal elements, (1) a step frequency spectrum analyzer, and (2) a wideband receiver. The step frequency spectrum analyzer has fifteen narrow-band frequency channels with center frequencies logarithmically spaced from 35 Hz to 100 kHz and one wide-band frequency channel with a bandpass of about 100 Hz to 10 kHz. The four highest frequency narrow-band filters of the step frequency analyzer have bandwidths of $\pm 7.5\%$ of their center frequencies

and the remaining narrow-band filters have bandwidths of $\pm 15.0\%$ of their center frequencies. A differential amplifier is used to provide a signal proportional to the potential difference between the antenna elements. The differential amplifier output signal drives all of the filters simultaneously. The filter outputs are then sequentially switched into an 80 db logarithmic detector to provide frequency spectrum measurements. The logarithmic detector output is a DC voltage proportional to the logarithm of the average input amplitude. The reprogrammable onboard data system controls the switching of the spectrum analyzer filters and the sampling of the logarithmic detector output.

The wideband receiver is an 80 db automatic gain control (AGC) receiver with a bandwidth of about 100 Hz to 10 kHz. The output of the wideband receiver modulates the special purpose telemetry transmitter. The wideband data is recorded on the ground and then processed by a spectrum analyzer to produce high resolution frequency-time spectrograms. The wideband system is normally operated one orbit out of three, but can be operated continuously for special periods.

III. OBSERVATIONS

Inbound orbit 99, during which Williams et al. [1972] reported the anomalous proton pitch angle distribution near the plasmopause boundary, occurred on December 17, 1971, during the initial phase of the magnetic storm. The apogee of this orbit was located at about 21.0 hours local time. Maynard and Cauffman [1972] have identified the inbound plasmopause crossing on this orbit from the DC potential difference between the spheres which changes abruptly at the plasmopause boundary. From their data, which are reproduced in panel (c) of Figure 1, they determined that the inbound plasmopause crossing on orbit 99 occurred at about 0615 UT and $L = 3.4$. Several features of the wide-band data which support this determination of the plasmopause location are discussed later in this paper.

Panel (d) of Figure 1 shows the electric field amplitudes for the eight lowest frequency channels (35 Hz to 1.78 kHz) near the inbound plasmopause crossing of orbit 99. The electric field amplitudes plotted are the peak RMS electric field amplitudes obtained over successive 67 second intervals. Peak values are shown in order to eliminate the modulation due to the spacecraft spin and to provide a quantitative indication of the amplitude of impulsive noise bursts which otherwise would not be as evident. The electric field amplitudes have been computed assuming that the effective length of the electric dipole antenna is equal to the separation distance between the spheres

(5.08 meters). Panels (a) and (b) of Figure 1 show frequency-time spectrograms of the wideband magnetic and electric fields, respectively.

Figure 1 shows that several features of the electric field noise change markedly near the plasmopause boundary at 0615 UT. In the 35 Hz and 62 Hz frequency channels it is evident that the electric field amplitudes decrease by more than an order of magnitude as the spacecraft crosses into the plasmasphere. Outside the plasmasphere at about 0600 UT the electric field amplitudes in the 35 Hz and 62 Hz channels are about $500 \mu\text{V (meter)}^{-1}$ and $100 \mu\text{V (meter)}^{-1}$, respectively, and inside the plasmopause at about 0616 UT the corresponding electric field amplitudes have decreased to about $30 \mu\text{V (meter)}^{-1}$ and $7.0 \mu\text{V (meter)}^{-1}$, respectively. Since similar changes have been observed both before and during a magnetic storm, this change in the electric field amplitudes in the 35 Hz and 62 Hz channels, and to a smaller extent in the 120 Hz channel, is apparently a characteristic feature of the plasmopause boundary and does not appear to be related to the occurrence of a magnetic storm except for the location of the plasmopause.

An even more pronounced enhancement in the low-frequency electric field noise, which is confined to the immediate vicinity of the plasmopause, is evident in Figure 1 between the vertical dashed lines at 0609:30 and 0615:40 UT. The maximum electric field amplitudes in the 62 Hz, 120 Hz, 200 Hz, and 311 Hz frequency channels during this period are nearly an order of magnitude greater than the corresponding amplitudes farther outside the plasmopause. A similar but smaller enhancement is also evident in the 562 Hz frequency channel.

Comparing these data with the $24.3 \text{ keV} \leq E \leq 35.1 \text{ keV}$ proton intensities reported by Williams et al. [1972] for this orbit, it is seen that this low-frequency electric field noise enhancement corresponds closely with the region of rapidly decreasing proton intensities and anomalous pitch angle distributions at the inner edge of the ring current.

Expanded 0 Hz to 650 Hz frequency-time spectrograms of the electric and magnetic fields near the plasmopause boundary are shown in Figure 2 for the period from 0614 to 0617 UT. The horizontal lines are ground based interference acquired during the recording and processing of the data. The large number of nearly vertical bursts of ~ 0.25 second or less duration extending until approximately 0615:40 UT in Figure 2 correspond to the enhanced low-frequency electric field noise intensities between the vertical dashed lines in Figure 1. These bursts are bunched in groups which last from a few seconds to several tens of seconds. The bursts occasionally extend to nearly 600 Hz, but are usually most intense below 300 Hz. The lower frequency cutoff at about 100 Hz is due to the lower frequency limit of the wideband receiver. These low-frequency noise bursts are not observed in the magnetic spectrogram (top panel of Figure 2) nor are they observed in the narrow-band data from the search coil magnetometer [Parady and Cahill, 1972]. Although the low-frequency noise bursts are most intense and rise to higher frequencies in the period from 0609:30 to 0615:40 UT the same type of noise bursts is also observed before 0609:30 UT. These low-frequency noise bursts have also been

observed on other orbits during this storm and have been either of much lower intensity or entirely absent during magnetically quiet periods.

Several features of the wideband data are similar to features found near the plasmopause by other satellites. In Figures 1 and 3 at 0615:33 UT, slightly inside the plasmopause (as determined by the GSFC electric field experiment), the first long hop whistler of this inbound pass is observed, similar to the results of Carpenter et al. [1969]. Further inside the plasmopause, at 0615:37 UT, an ELF hiss band is observed corresponding to the "plasmaspheric hiss" discussed by Russell and Holzer [1970] and Carpenter et al. [1969]. As seen from Figure 2 this ELF hiss emission is confined to a narrow frequency band from about 300 Hz to 420 Hz. These frequency limits do not vary for the entire time of observation which suggests that the noise is being generated at a specific point and then propagating to other regions. As seen in panel (d) of Figure 1, the electric field strength in the 311 Hz frequency channel is $50 \mu\text{V (meter)}^{-1}$ at 0616 UT, increases to $580 \mu\text{V (meter)}^{-1}$ at 0618 UT, and slowly decreases to $26 \mu\text{V (meter)}^{-1}$ at 0646 UT. As can be seen in Figure 2, the amplitude of the ELF hiss has a pronounced spin modulation. The nulls in the magnetic field intensity occur when the search coil axis is perpendicular to the geomagnetic field. The nulls in the electric field intensity occur when the electric dipole axis is parallel to the geomagnetic field. This field geometry implies that the ELF hiss is propagating nearly perpendicular to the geomagnetic field. We are currently attempting

to determine the Poynting flux direction of this noise from the relative phase of the electric and magnetic antenna signals.

At higher frequencies, above about 1 kHz, the predominant phenomena observed outside the plasmopause is banded chorus of the type described by Burtis and Helliwell [1969]. Several sporadic bursts of banded chorus are evident in panel (b) of Figure 1 prior to 0556 UT at a frequency of about 4 kHz. Later two well-defined bands of banded chorus are evident. The lower frequency band begins at about 0605 UT and ends at about 0615 UT. The higher frequency band begins at about 0602 UT and moves out of the passband of the wideband receiver at 0618 UT. The frequency of these bands increases systematically with decreasing altitude. In the on-board spectrum analyzer data the higher band is observed in the 10.0 kHz ($\pm 15\%$) frequency channel until 0627 UT and in the 16.5 kHz ($\pm 7.5\%$) frequency channel at 0632 UT. The center frequency of the lower frequency band is about 0.27 of the measured local electron cyclotron frequency from 0605 to 0615 UT. The center frequency of the higher frequency band is about 0.36 of the measured local electron cyclotron frequency from 0602 to 0618 UT. The frequency-time character of the discrete emissions which form these bands is illustrated in the expanded time scale spectrograms of Figures 3 and 4. The lower band consists of nearly vertical emissions of 0.25 second or less in duration with a bandwidth of about 1 kHz. Before about 0614 UT the higher band consists of intense vertical bursts similar to those in the lower band; however, these bursts are followed by a rising diffuse noise of about 1 second duration

as can be seen in Figure 4. Beginning at about 0615 UT the intense vertical bursts disappear and the higher band consists only of diffuse noise in the same frequency range where the vertical bursts previously occurred. Banded chorus has been observed on most passes which go outside of the plasmasphere.

To summarize the electric field noise intensities observed during orbit 99 the electric field spectral densities measured by S³-A over the frequency range from 1 Hz to 100 kHz are shown in Figure 5 for three representative locations: (1) outside of the plasmasphere at $L = 3.87$, (2) near the plasmopause at $L = 3.44$, and (3) inside the plasmasphere at $L = 3.30$. The data from 1 Hz to 30 Hz were provided by Nelson Maynard from the GSFC electric field experiment on S³-A. Above about 1 kHz the electric field spectral densities do not vary greatly across the plasmopause except for the occurrence of banded chorus near and outside the plasmopause. With the exception of the ELF hiss band at about 300 Hz the electric field spectral densities at frequencies below about 1 kHz are generally much larger outside the plasmopause than inside. At frequencies below about 100 Hz this large increase in the electric field intensity outside of the plasmopause may be partly attributed to harmonics of the spacecraft spin rate which are generated by asymmetrical spacecraft sheath effects outside of the plasmopause. Near the plasmopause (at $L = 3.44$ in Figure 5) the main contribution to the broadband electric field strength comes from the broad peak in the electric field spectral density which extends from about 20 Hz to 500 Hz with a maximum at about 62 Hz.

This enhancement is produced by the low-frequency electric field noise bursts shown in Figure 2. The maximum integrated RMS electric field strength for these low-frequency noise bursts is about 1 mV (meter)⁻¹.

IV. DISCUSSION

The most striking and unusual feature of these storm time electric field observations is the occurrence of a region of intense low-frequency electric field noise bursts just outside the plasmopause boundary. These electric field noise bursts, which extend from about 20 Hz to 500 Hz, are purely electrostatic and appear to be closely related to the occurrence of a magnetic storm, since no comparable noise bursts have been found during magnetically quiet periods. These noise bursts occur at the inner boundary of the proton ring current and in the region of anomalous proton pitch angle distribution reported by Williams et al. [1972]. The spatial correspondence between these two phenomena suggests that this electrostatic noise may be responsible for the pitch angle scattering and loss of ring current protons from the region near the plasmopause boundary during this storm. Nagy et al. [1972] have also reported a similar enhancement in the low-frequency (4 Hz to 256 Hz) electric field intensities in association with an SAR-Arc at low altitudes near the plasmopause boundary. These low-frequency noise bursts may possibly be related to the electrostatic plasma instability described by Coroniti et al. [1972]. The frequency range of this instability, which is between the ion cyclotron frequency and the ion plasma frequency, agrees reasonably well with the observed frequency range of the electric field noise bursts. The electric field

amplitudes estimated by Coroniti et al. [1972] for this instability, 10 to 100 mV (meter)⁻¹, are however significantly larger than the broad band amplitudes, ~ 1 mV (meter)⁻¹, which have been observed for this noise.

ACKNOWLEDGMENTS

We wish to thank Drs. Laurence J. Cahill, Jr. and Nelson C. Maynard for letting us use their data in this paper.

This research was supported in part by the National Aeronautics and Space Administration under Contract NAS5-11167 and Grant NGL-16-001-043 and the Office of Naval Research under Grant N00014-68-A-0196-0003.

REFERENCES

- Burtis, W. J. and R. A. Helliwell, Banded chorus -- a new type of VLF radiation observed in the magnetosphere by OGO 1 and OGO 3, J. Geophys. Res., 74, 3002, 1969.
- Carpenter, D. L., C. G. Park, H. A. Taylor, Jr., and H. C. Brinton, Multi-experiment detection of the plasmopause from EOGO satellites and Antarctic ground stations, J. Geophys. Res., 74, 1837, 1969.
- Cornwall, J. M., F. V. Coroniti, and R. M. Thorne, Turbulent loss of ring current protons, J. Geophys. Res., 75, 4699, 1970.
- Cornwall, J. M., F. V. Coroniti, and R. M. Thorne, Unified theory of SAR arc formation at the plasmopause, J. Geophys. Res., 76, 4428, 1971.
- Coroniti, F. V., R. W. Fredricks, and Roscoe White, Electrostatic instability of ring current protons beyond the plasmopause during injection events, Research Report 22935-6001-R0-00, Space Sciences Department, TRW Systems Group, Redondo Beach, California, May 1972.

Maynard, N. C. and D. P. Cauffman, Double floating probe measurements on S³-A, J. Geophys. Res., submitted for publication, 1972.

Nagy, A. F., W. B. Hanson, T. L. Aggson, and R. J. Hoch, Satellite and ground-based observations of a red arc, J. Geophys. Res., 77, 3613, 1972.

Parady, B. and L. J. Cahill, Jr., ELF observations during the December 1971 storm, J. Geophys. Res., submitted for publication, 1972.

Russell, C. T. and R. E. Holzer, AC magnetic fields, in Particles and Fields in the Magnetosphere, edited by B. M. McCormac, p. 195, D. Reidel Publishing Co., Dordrecht, Holland, 1970.

Williams, D. J., T. A. Fritz, and A. Konradi, Observations of proton spectra ($0.6 \leq E \leq 300$ keV) and pitch angle distributions at the plasmopause, J. Geophys. Res., submitted for publication, 1972.

FIGURE CAPTIONS

Figure 1 Four sets of field observations for inbound orbit 99 in the vicinity of the plasmopause. All four panels contain data for the same 56 minute time period from 0550 to 0646 UT on December 17, 1971. Panel (a) is a 0 Hz to 3 kHz frequency-time spectrogram of the magnetic wideband data from the University of Minnesota's Search Coil Magnetometer Experiment. Panel (b) is a 0 Hz to 10 kHz frequency-time spectrogram of the University of Iowa's Electric Field Experiment wideband data. Panel (c) is a plot of the DC potential difference between the spheres measured by the Goddard Space Flight Center's Electric Field Experiment. Panel (d) contains plots of the amplitudes measured for the eight lowest frequency channels of the University of Iowa's Electric Field Experiment onboard spectrum analyzer. The peak RMS amplitudes for 67 second intervals of time are plotted. The region between the dashed lines is where the enhancement in the low-frequency electric field noise is most intense.

Figure 2 The upper panel is a 0 Hz to 650 Hz frequency-time spectrogram of the magnetic field wideband data. The lower

panel is a 0 Hz to 650 Hz frequency-time spectrogram of the electric field wideband data. Both panels are for the same three minute period near the plasmopause. Note that the intense vertical bursts from 0614 to 0615:40 UT occur only in the electric field data. The ELF hiss band from about 300 Hz to 420 Hz which begins at 0615:37 UT is present in both the electric and the magnetic field data. Analysis of the spin modulation of the ELF hiss band determined that the hiss is propagating nearly perpendicular to the geomagnetic field. The ELF hiss band has the same well defined frequency limits for more than 30 minutes as the satellite moves inward more than $1 R_E$.

Figure 3 A 0 Hz to 10 kHz frequency-time spectrogram of the electric field wideband data near the plasmopause. The first whistler on inbound orbit 99 is observed at 0615:33 UT just inside the plasmopause. The ELF hiss band described in Figure 2 begins shortly after the whistler observation. The low-frequency electric field noise bursts, which are most intense from 0615:10 to 0615:35 UT, are shown expanded in frequency in Figure 2. Banded chorus is observed above 8.5 kHz and consists of a band of diffuse noise bursts in contrast to that observed in Figure 4 only 4 minutes earlier.

Figure 4 A 0 Hz to 10 kHz frequency-time spectrogram of the electric field wideband data just outside the plasmopause. Intense low-frequency noise bursts are evident up to 500 Hz for tens of seconds. The discrete emissions near 6.0 kHz and 8.0 kHz are banded chorus. The upper band has diffuse noise following each emission. In Figure 3 just 4 minutes later only diffuse noise above 8.5 kHz is present.

Figure 5 The electric field spectral density from 1 Hz to 100 kHz for measurements made outside the plasmasphere at $L = 3.87$, near the plasmopause at $L = 3.44$, and inside the plasmasphere at $L = 3.30$. The broad peak from 20 Hz to 500 Hz for $L = 3.44$ is a result of the low-frequency electric field noise bursts shown in Figure 2. The maximum integrated rms electric field strength for these noise bursts is about $1 \text{ mV (meter)}^{-1}$. Below 200 Hz the electric field spectral density is significantly larger outside the plasmasphere than inside the plasmasphere.

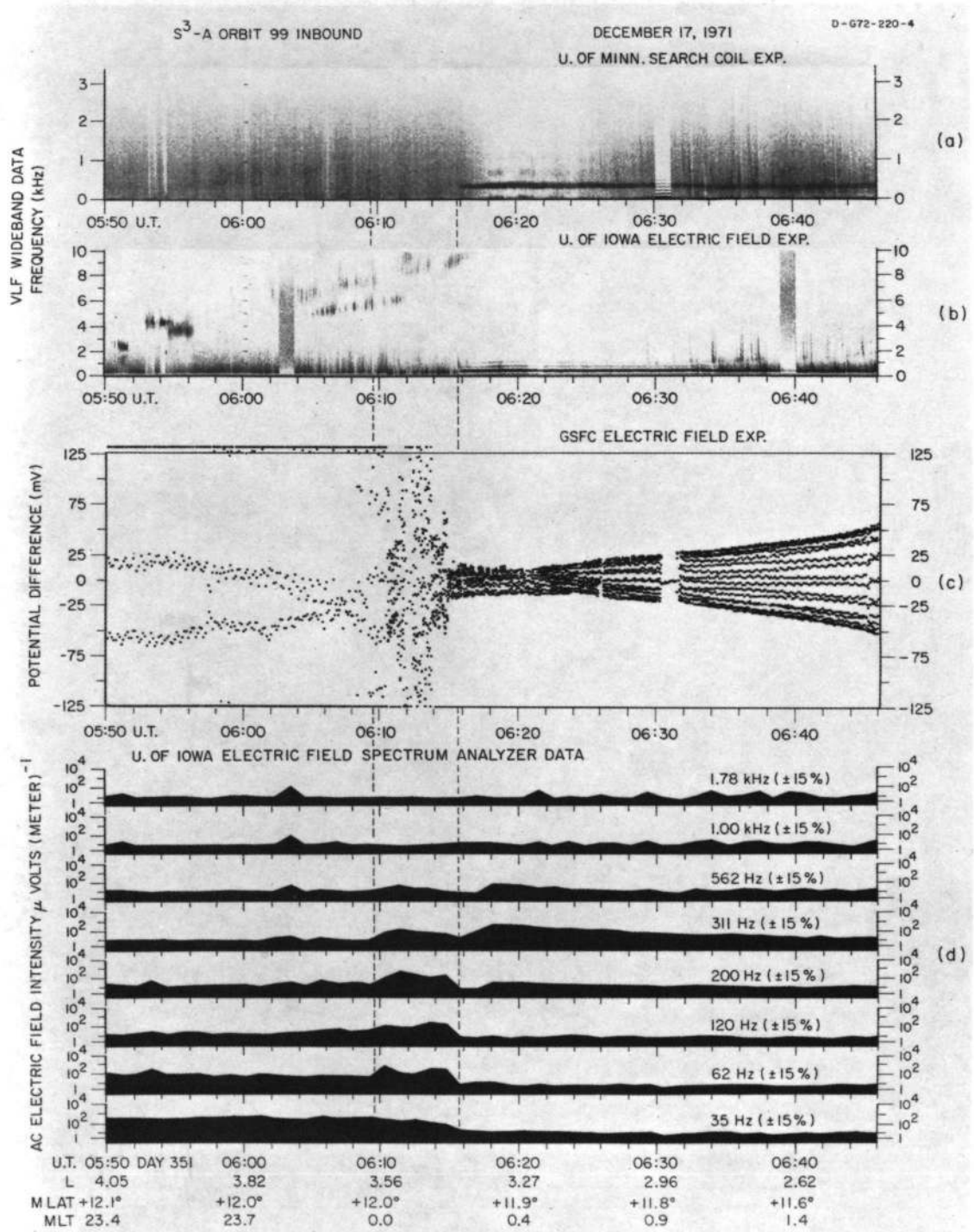


Figure 1

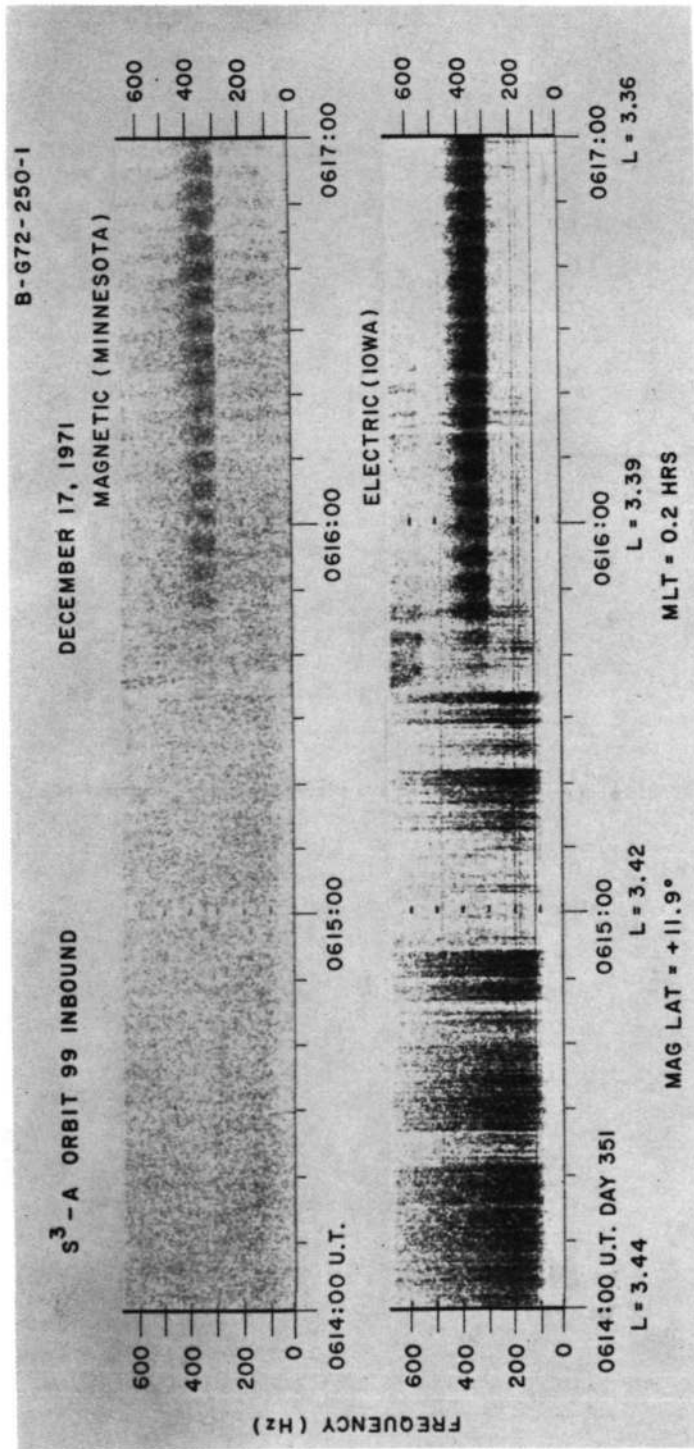


Figure 2

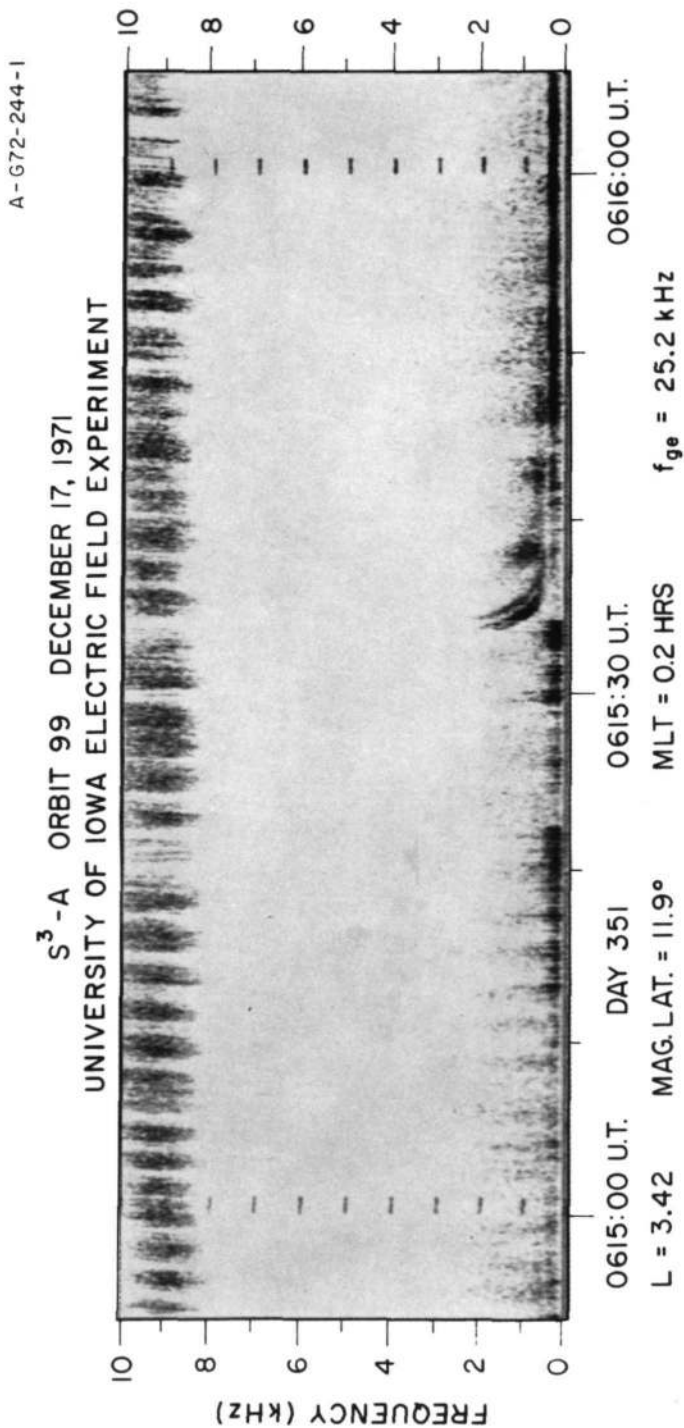


Figure 3

A-672-243-1

S³-A ORBIT 99 DECEMBER 17, 1971
UNIVERSITY OF IOWA ELECTRIC FIELD EXPERIMENT

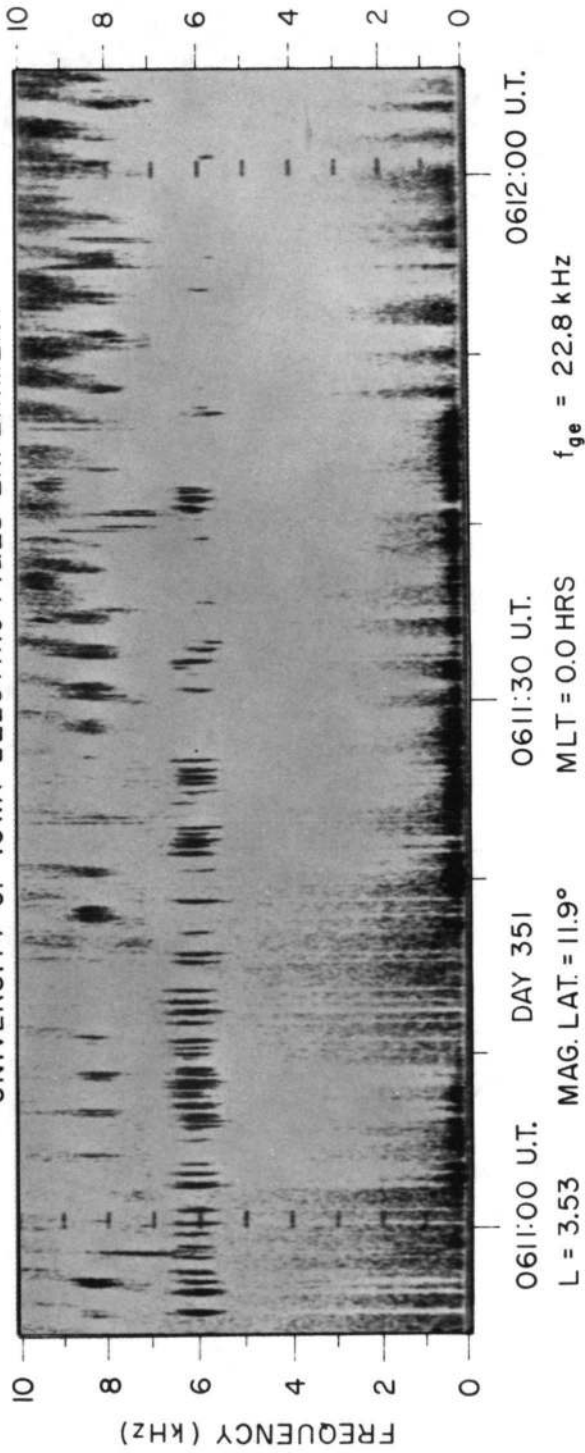


Figure 4

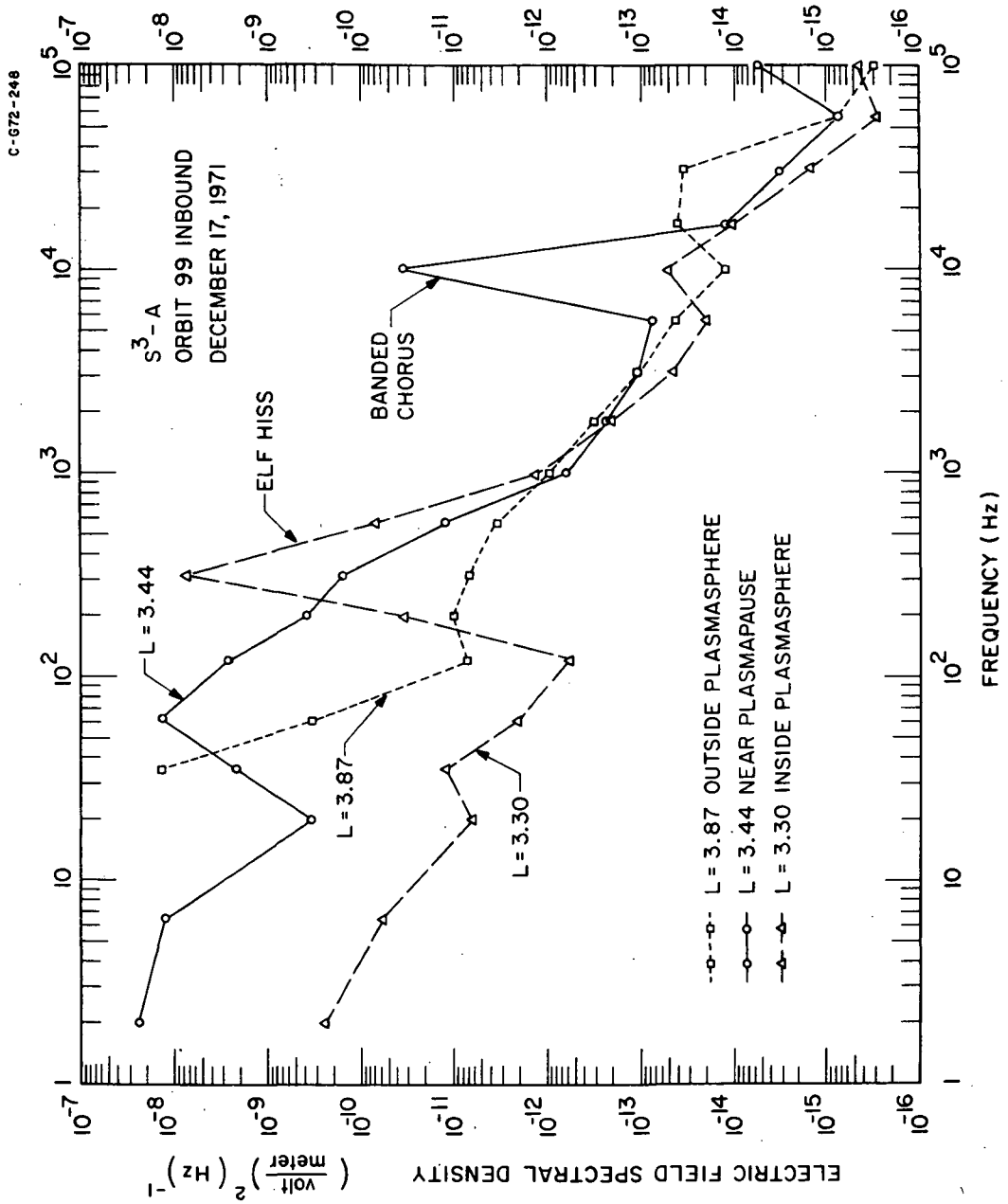


Figure 5